Electronic Supplementary Information (ESI) for:

Acceptor defect participating magnetic exchange in ZnO:Cu nanocrystalline film: defect structure evolution, Cu-N synergetic role and magnetic control

Liang Hu, Liping Zhu,* Haiping He,* Le Zhang and Zhizhen Ye

State Key Laboratory of Silicon Materials, Department of Materials Science and Engineering, Zhejiang University, Hangzhou 310027, P. R. China

Cyrus Tang Center for Sensor Materials and Applications, Zhejiang University, Hangzhou 310027, P. R. China

E-mail: zlp1@zju.edu.cn, hphe@zju.edu.cn; Fax: +86-571-87952625; Tel: +86-571-87951958

Graphic and Tabular Lists

lightly-doped (0.8%) and heavily-doped (2.0%) samples.

Figure S7 A series of FT-IR spectra recorded from amine-bath-treated, amine-bath-untreated and amine-annealed ZCO4.0 NCs.

Figure S8 The corresponding variation of C 1s XPS binding environment in ZCO4.0 NCs processed by different conditions.

Figure S9 Room-temperature ESR signal of free diluted Cu^{2+} ions in chloroform solution.

Figure S10 The comparison of 300 K PL spectra recorded from N-capped ZnO NC film before and after vacuum treatment.

Figure S11 300 K magnetization from OA-capped 0.2% Cu-doped ZnO colloidal NCs, a spin-coated NC film without OA capping, annealed at 400°C, and the same NC film with OA capping.

Figure S12 300 K ESR signals of pure ZnO NCs (without OA capping) before and after aggregation.

Figure S13 300 K magnetization contrast between spin-coated ZnO NC film before and after OA capping, annealed at 400°C.

Figure S14 The effect of amine-capping on texture in 400°C annealed 0.2% Cu-doped ZnO nanocrystalline film.

Figure S15 The effect of amine-capping on grain-size in 400°C annealed 0.2% Cu-doped ZnO nanocrystalline film.

Figure S16 The effect of amine-capping on amorphous layer in 400°C annealed 0.2% Cu-doped ZnO nanocrystalline film.

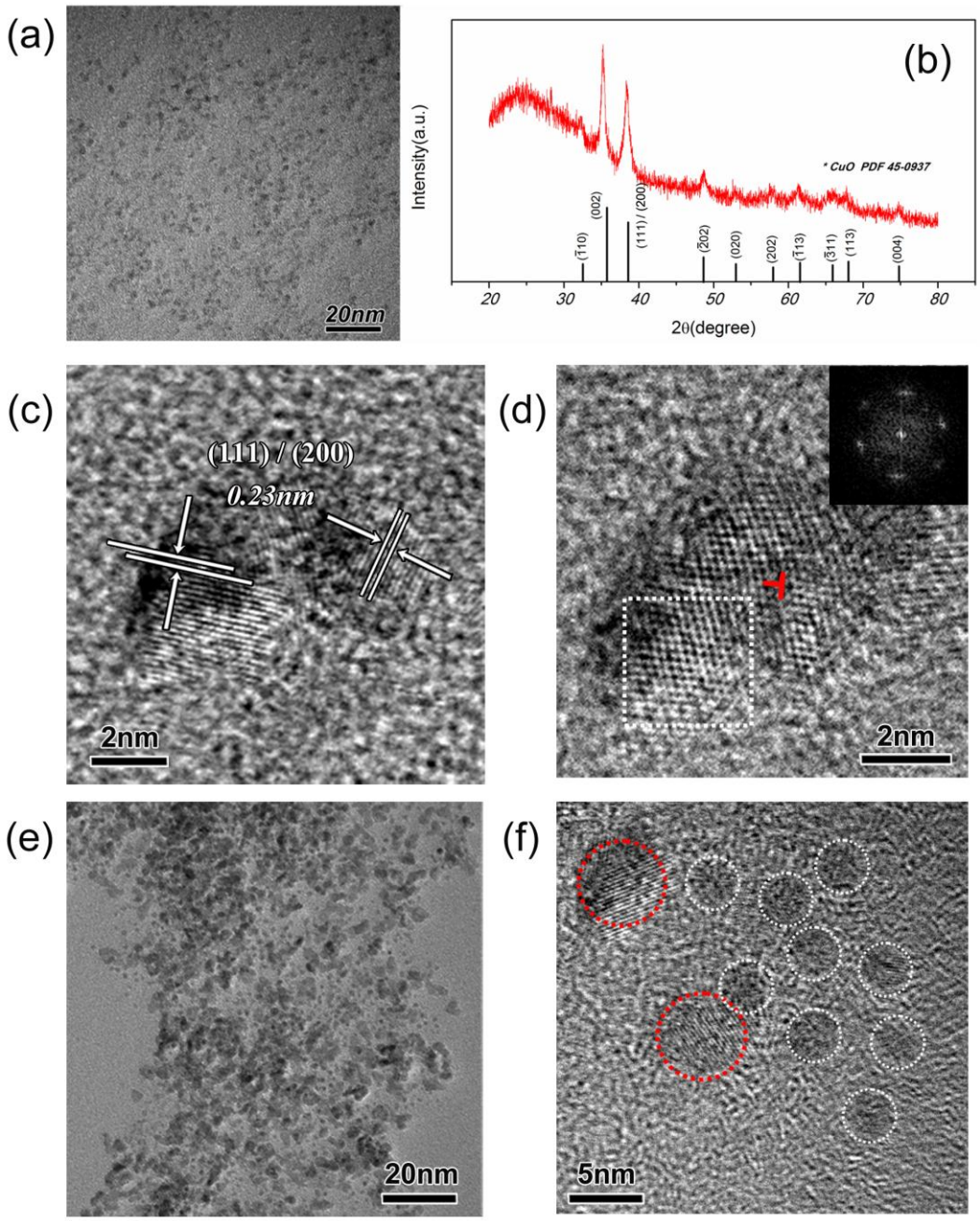

Fig. S1 (a), (b), and (c) represent TEM image, XRD profile, and HRTEM image of home-made pure CuO NCs, respectively. For comparison, highly-doped ZnO:Cu (8%) NCs including CuO secondary phase are shown in (d-f). Among them, (e) is survey TEM, (d) and (f) are the magnified images. Small particles circled by white dashed-line in (f) indicate CuO NCs, while red ones represent doped ZnO NCs.

Table S1. Details of the preparing method, copper doping amount, and magnetic parameters (saturated magnetization M_s, coercivity H_c, and Curie temperature T_c) for different ZnO:Cu sample types in terms of powder and film.

Material type	Preparing method	Doping amount (at.%)	M_s (μ_B/Cu)	H_c (Oe)	T_c (K)	Ref.
Powder[a]	CVD[b]	2.2%	1.48	-	380	1
	CVD	1.37%	0.2	50	-	2
	sol-gel	5%	2.6×10^{-4}	-	-	3
	sol-gel	2%	PM[g]	0	-	4
	sol-gel	3%	0.4	-	-	5
	hydrothermal	0.5%	0.47	47	-	6
	hydrothermal	1%	0.001	1500	-	7
	thermal diffusion	4.9%	0.074	-	-	1
	thermal diffusion	< 1%	1.39	>1000	-	8
	vapor transport	0.5%	0.116	-	-	9
	vapor transport	1%	0.2	100	300	10
	coprecipitation	5%	7.3×10^{-6}	-	300	11
	solvothermal	1.86%	0.013	400	400	12
	ion implantation	2%	0.42	752	300	13
Film	FCVA[c]	2.4%	0.037	<1000	-	14
	FCVA (N_2O annealing)	1.3%	0.73	81	-	15
	FCVA (Zn annealing)	1.3%	0.4	-	-	16
	PLD[d]	< 5%	0.18	-	-	17
	PLD	5%	0.81	100	320	18
	PLD	5%	1.45	1875	-	19

	PLD	2%	0.75	-	-	20
	PLD	2%	0.75	61	300	21
	PLD	2%	0.5	260	750	22
	PLD	1%	0.4	-	400	23
	PVD[e]	5%	0.14[h]	100	-	24
	MS[f]	< 3%	1.62	168	350	25
	MS	2%	1.8	-	350	26
	MS	5%	0.52	-	360	27
	MS	2.5%	0.25	-	300	28
	MS	0.6%	1.6	50	300	29
	hydrothermal	2%	0.4	-	-	30
	RF plasma deposition	8%	0.03	-	-	31

Note:

a: including any shape nanopowders or substrate-supported nanostructures

b: chemical vapor deposition

c: filtered cathodic vacuum arc technique

d: pulsed laser deposition

e: physical vapor deposition

f: magnetron sputtering

g: paramagnetism

h: emu/cm^3 (unit)

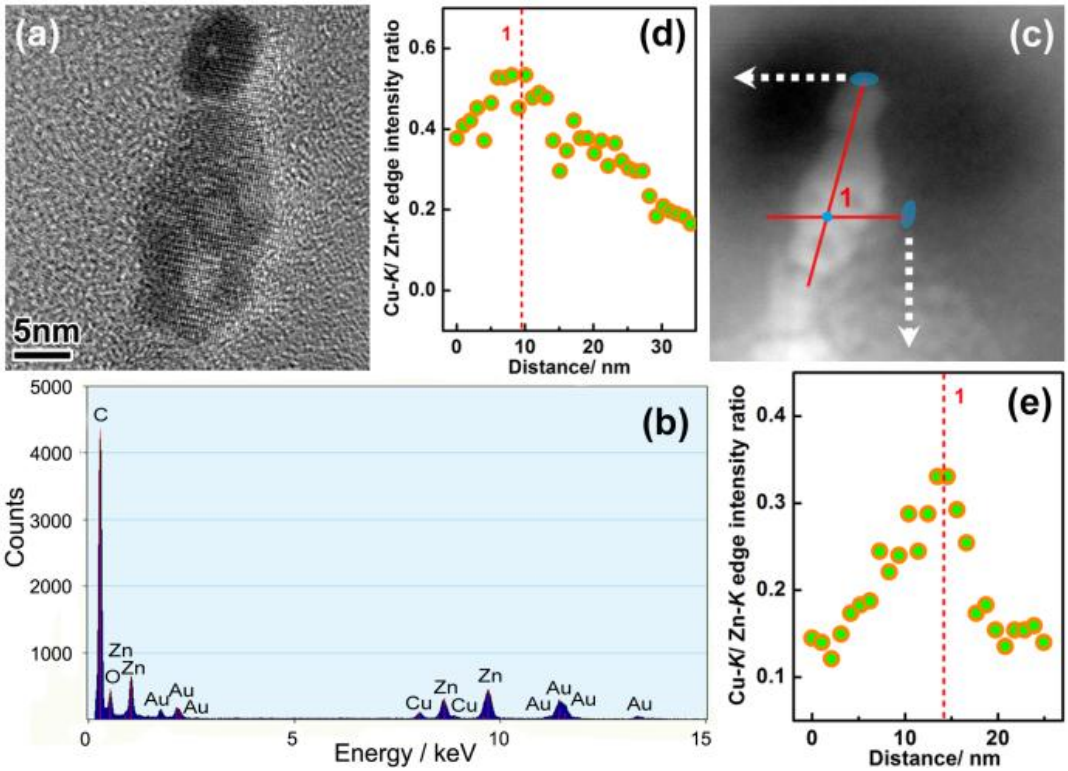

Fig. S2 STEM and EDX results of a single N-capped ZCO0.8 nanoparticle. (a) Original HRTEM image. (b) EDX spectrum suggesting the presence of Zn, Cu and O elements. (c) Corresponding HAADF-STEM image. The observed contrast difference corresponds to the dopant distribution inhomogeneity. (d-e) Line-scan EDX results of Cu *K*-edge/ Zn *K*-edge intensity ratio from different scan directions. The fact that the maximum intensity ratio is around the middle of the NC, could be well understood because the sample thickness there is the largest.

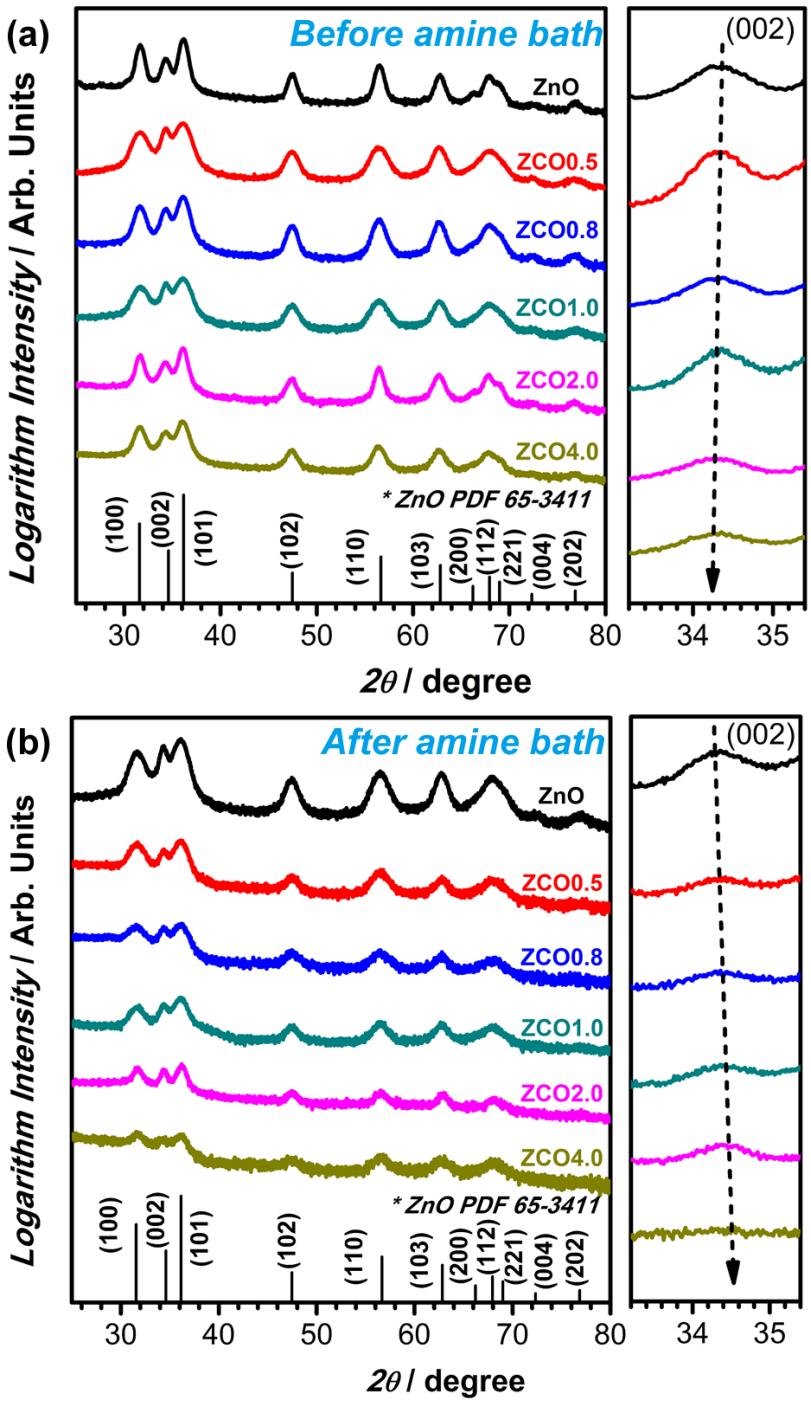

Fig. S3 XRD data of as-prepared ZnO:Cu NCs (a) before and (b) after amine bath treatment. In each figure, on the right panel, a continuous shift of (002) diffraction peak was extracted for observing dopant-induced lattice expansion or contraction. After amine bath, the diffraction peak width slightly turns larger, which possibly stems from more dispersive NC distribution due to OA ligand modification.

Table S2. Detailed XRD refinement result from Rietveld Analysis Program (Orion Software)

	Doping amount/ at.%	*d*(002)/ Å	*d*(101)/ Å	*a*/ Å	*c*/ Å
ZnO:Cu NCs without amine bath	0	2.603(4)	2.475(7)	3.246(6)	5.206(9)
	0.5	2.603(7)	2.475(9)	3.249(5)	5.207(5)
	0.8	2.607(9)	2.478(4)	3.254(1)	5.215(9)
	1.0	2.611(0)	2.483(0)	3.259(2)	5.221(9)
	2.0	2.611(9)	2.484(2)	3.260(9)	5.223(8)
	4.0	2.616(1)	2.489(3)	3.268(0)	5.232(1)
ZnO:Cu NCs with amine bath	0	2.603(8)	2.475(4)	3.248(9)	5.207(6)
	0.5	2.602(9)	2.469(6)	3.239(4)	5.205(7)
	0.8	2.602(3)	2.469(3)	3.239(1)	5.204(5)
	1.0	2.600(9)	2.468(7)	3.238(6)	5.201(8)
	2.0	2.597(6)	2.467(9)	3.238(4)	5.195(2)
	4.0	2.588(6)	2.466(7)	3.239(1)	5.177(1)

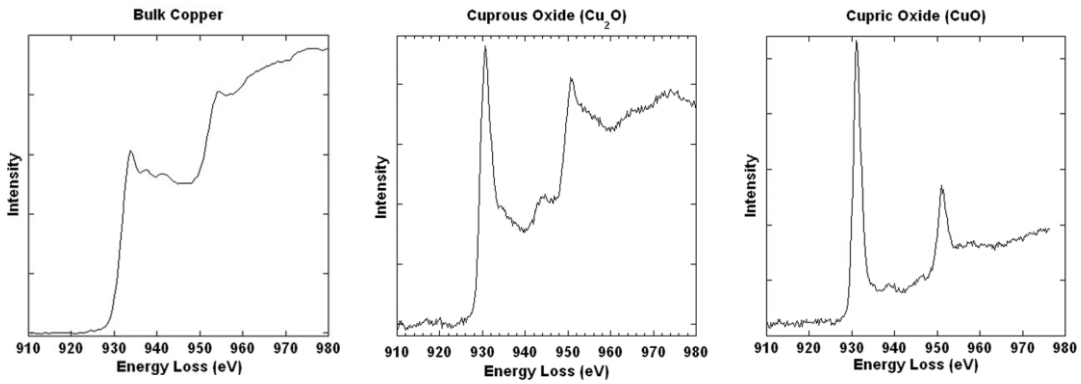

Fig. S4 EELS reference signals collected from home-made pure-phase Cu, Cu_2O and CuO nanoparticles.

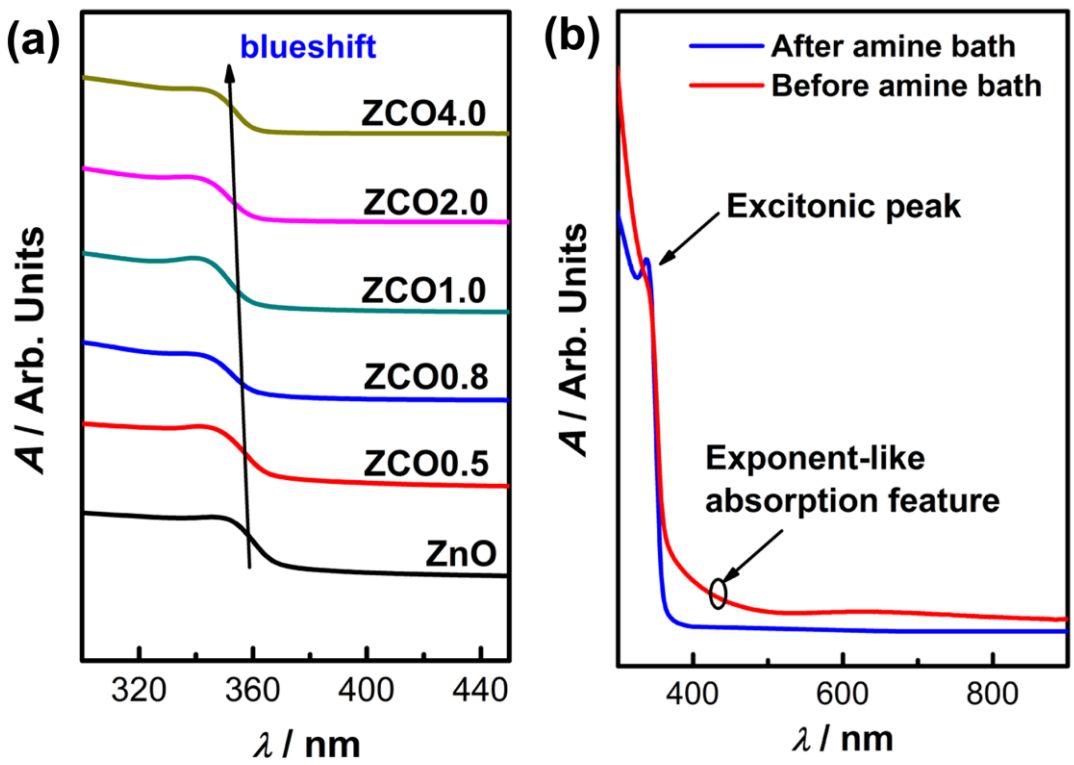

Fig. S5 (a) Dopant concentration-dependent excitonic absorption spectra. (b) An absorption spectral comparison of ZCO0.8 samples before and after amine bath treatment. Exponent-like feature of absorption spectrum in the whole visible range of NCs without amine bath indicates a sort of continuous energy-level structure, supportive of the presence of atomic Cu metal. Through amine bath processing, this band-like structure will disappear, implying the transformation of copper atom local environment.

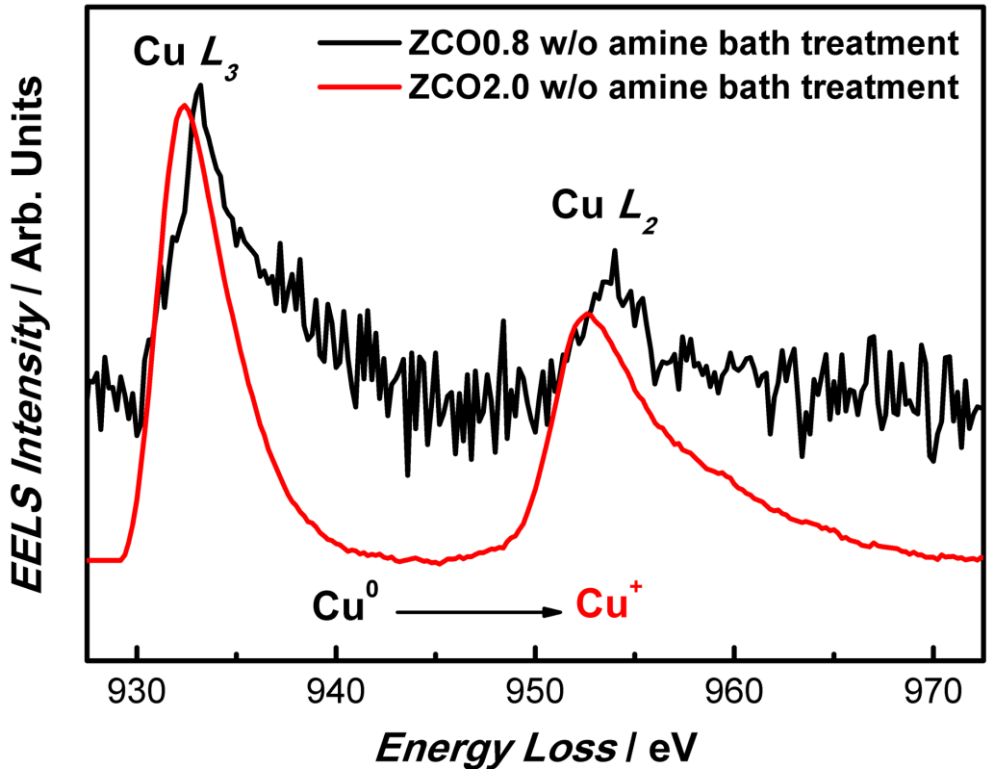

Fig. S6 The Cu $L_{3,2}$ core-loss EELS comparison between amine-bath-untreated lightly-doped (0.8%) and heavily-doped (2.0%) samples.

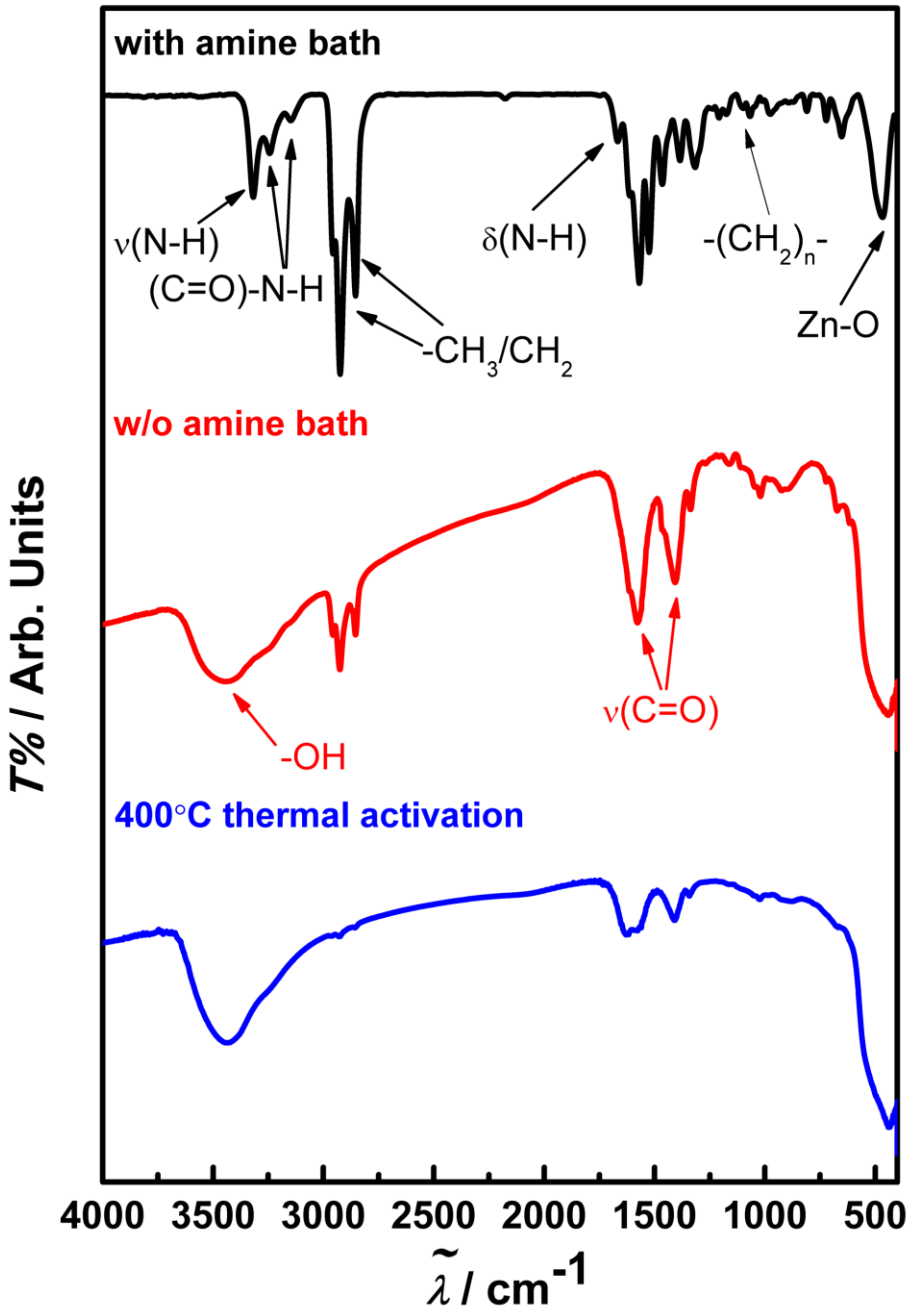

Fig. S7 A series of FT-IR spectra recorded from amine-bath-treated, amine-bath-untreated and amine-annealed ZCO4.0 NCs. The disappearance of O–H stretching vibration in amine-bath-treated sample indicates a charge transfer interaction between donor-like hydroxyl and Cu acceptor. Not only this, with ligand thermal decomposition at 400°C, all amine molecule related vibrations have disappeared, indicating N atoms have diffused into the bulk of ZnO:Cu.

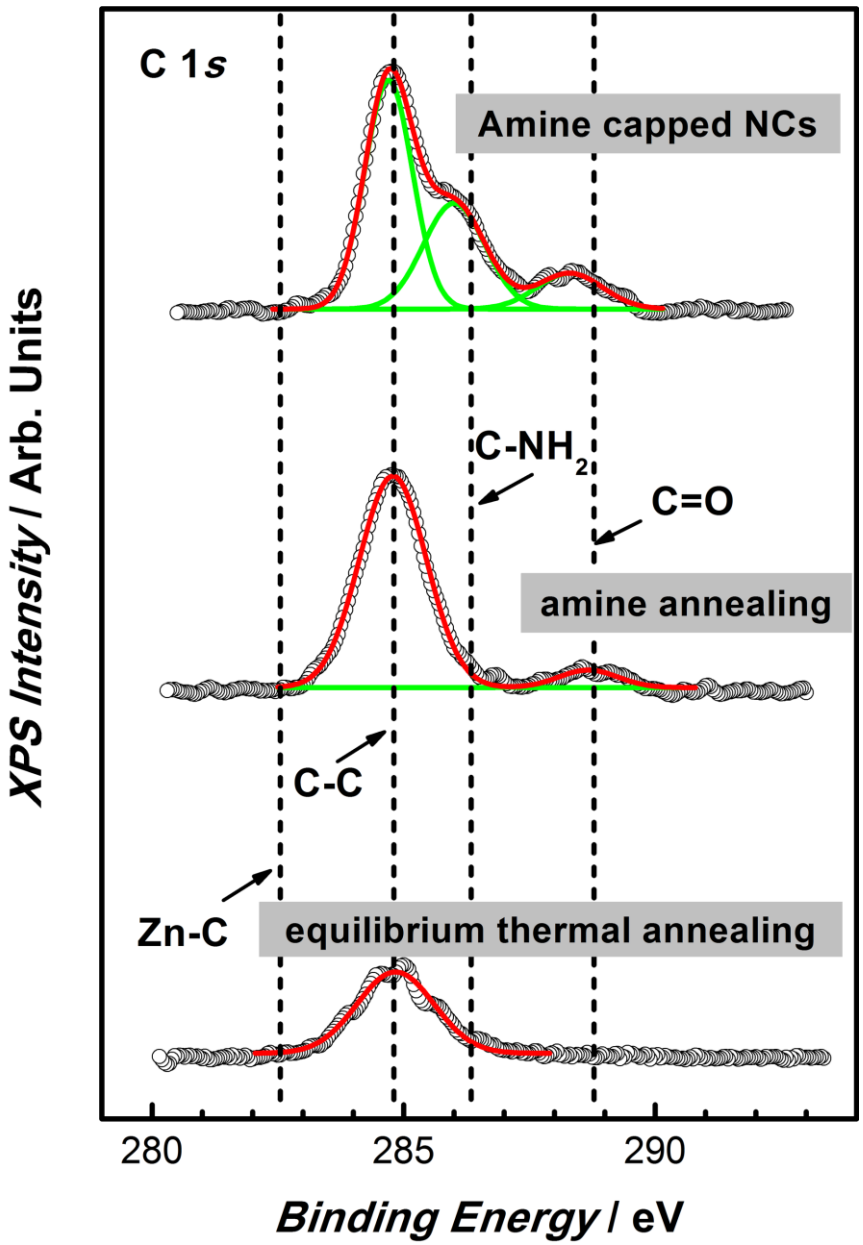

Fig. S8 The corresponding variation of C 1*s* XPS binding environment in ZCO4.0 NCs processed by different conditions. For different samples, the aim of element analysis is distinct. C 1*s* analysis of both amine-processed samples should be done only on the surface part. Since OA molecules have diffused into the bulk in annealing, surface C-N bonds should be non-available, which has been confirmed by this figure. Different from the above samples, the one annealed at 600°C in equilibrium was scanned after Ar^+ ions surface etching (etching depth ca.10 nm) in order to monitor possible carbon contamination effect and exclude the possibility of Zn-C bond for FM contribution.

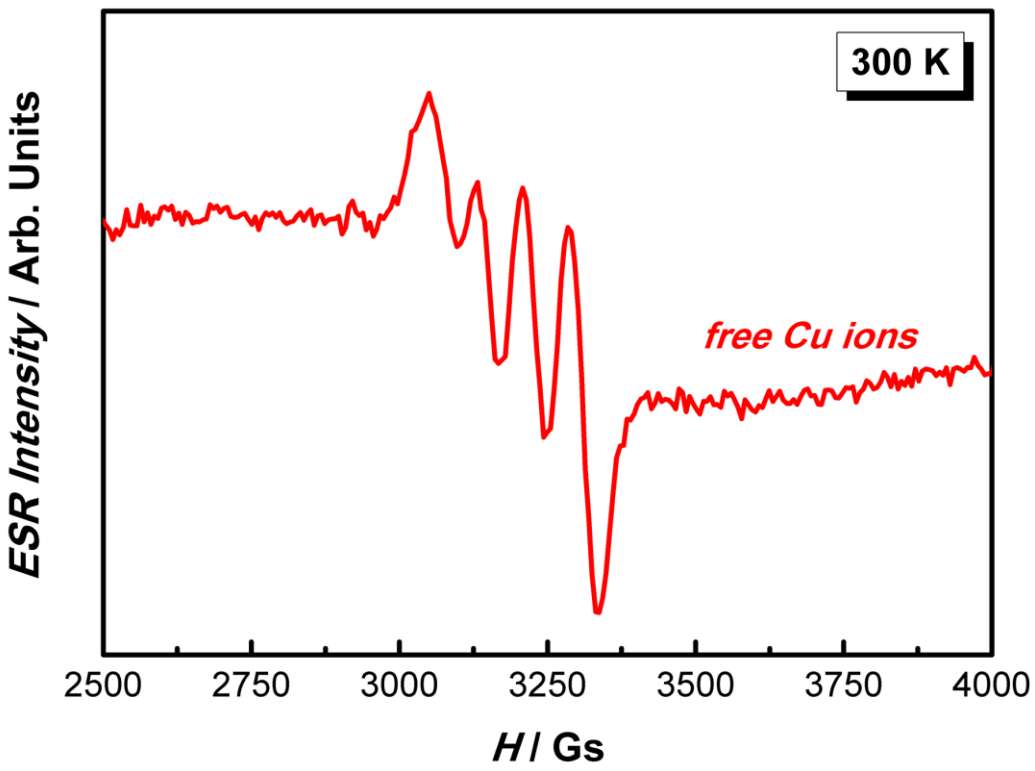

Fig. S9 Room-temperature ESR signal of free diluted Cu^{2+} ions in chloroform solution.

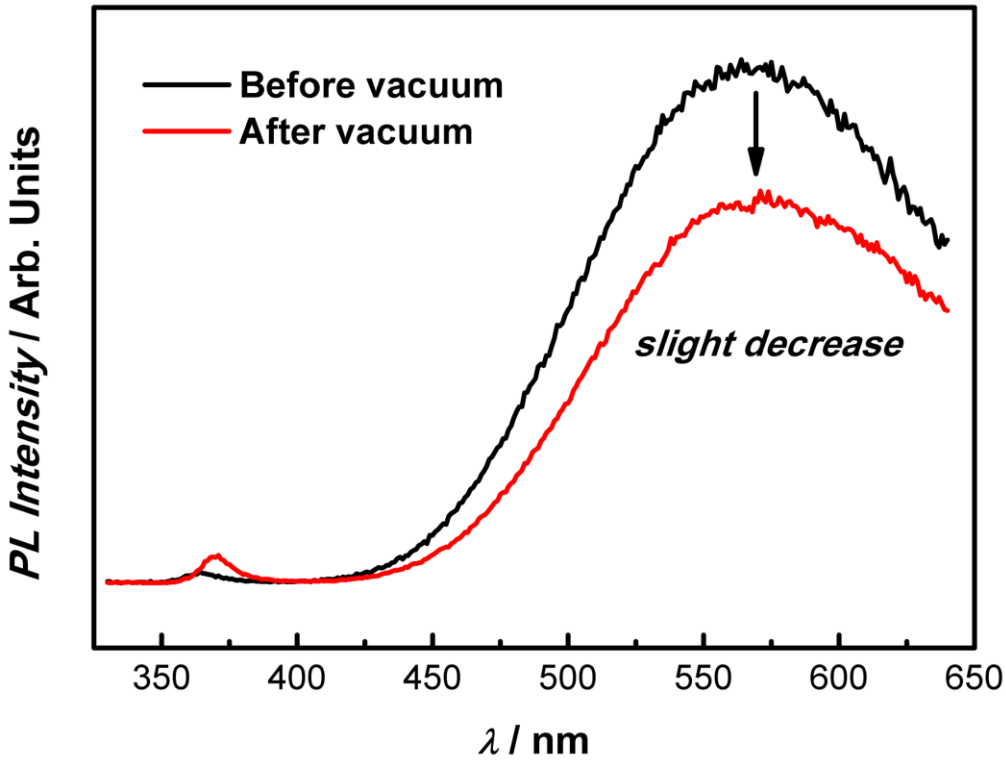

Fig. S10 The comparison of 300 K PL spectra recorded from N-capped ZnO nanocrystalline film before and after vacuum treatment.

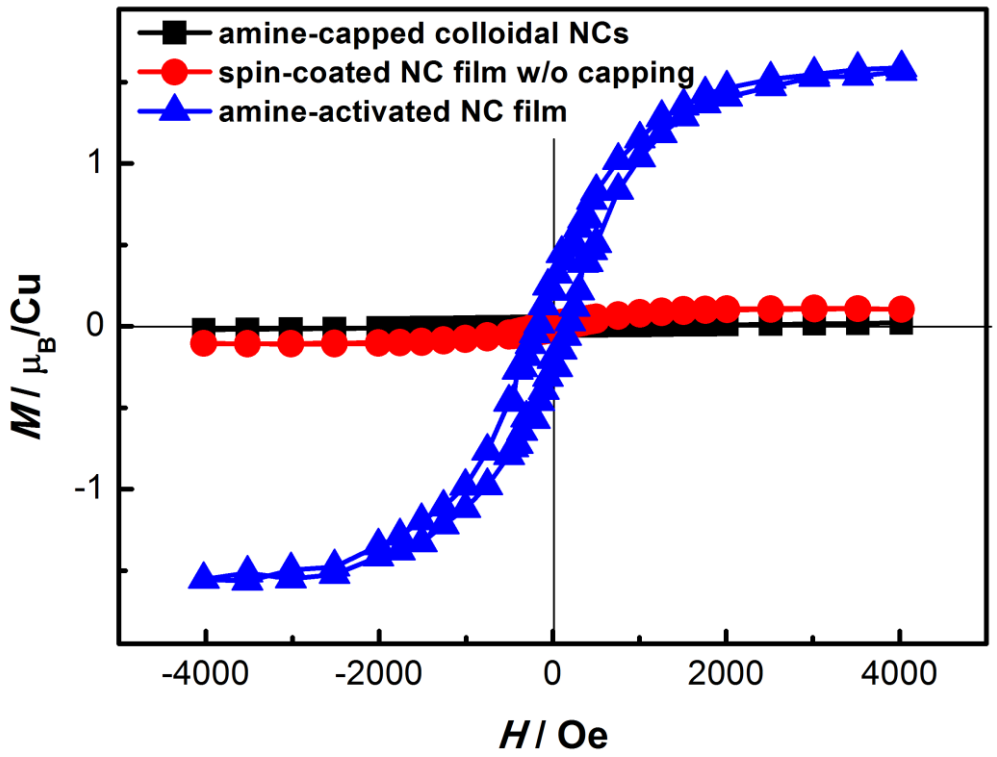

Fig. S11 300 K magnetization from OA-capped 0.2% Cu-doped ZnO colloidal NCs, a spin-coated NC film without OA capping, annealed at 400°C, and the same NC film with OA capping. All data have been corrected for a diamagnetic background.

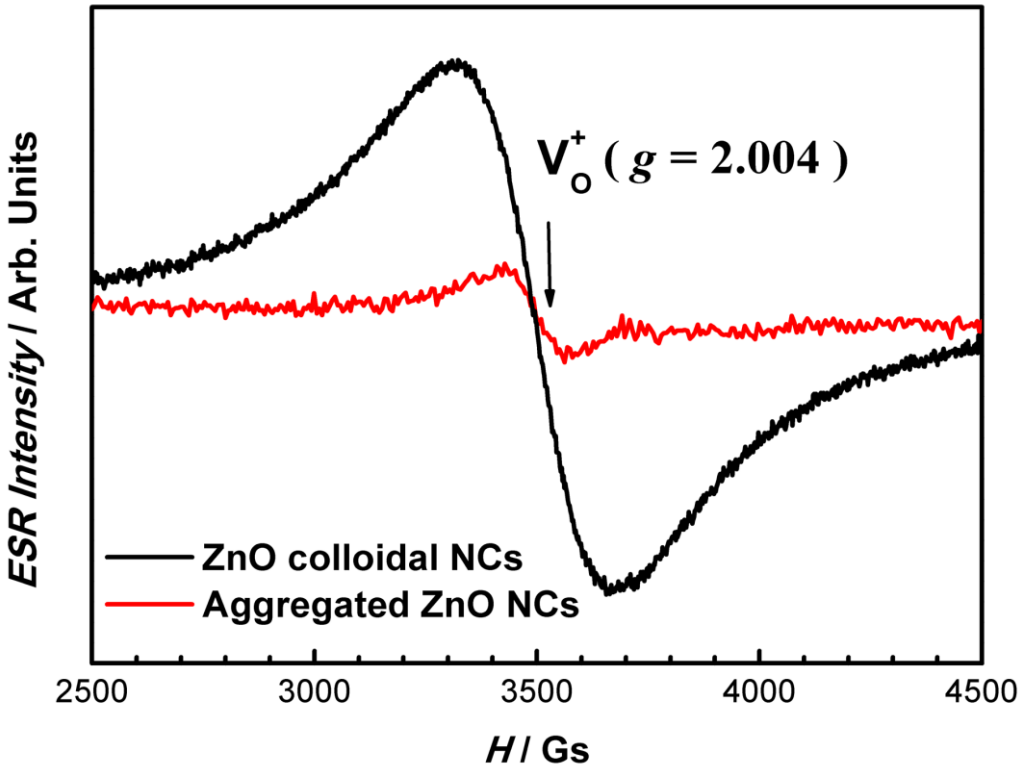

Fig. S12 300 K ESR signals of pure ZnO NCs (without OA capping) before and after aggregation.

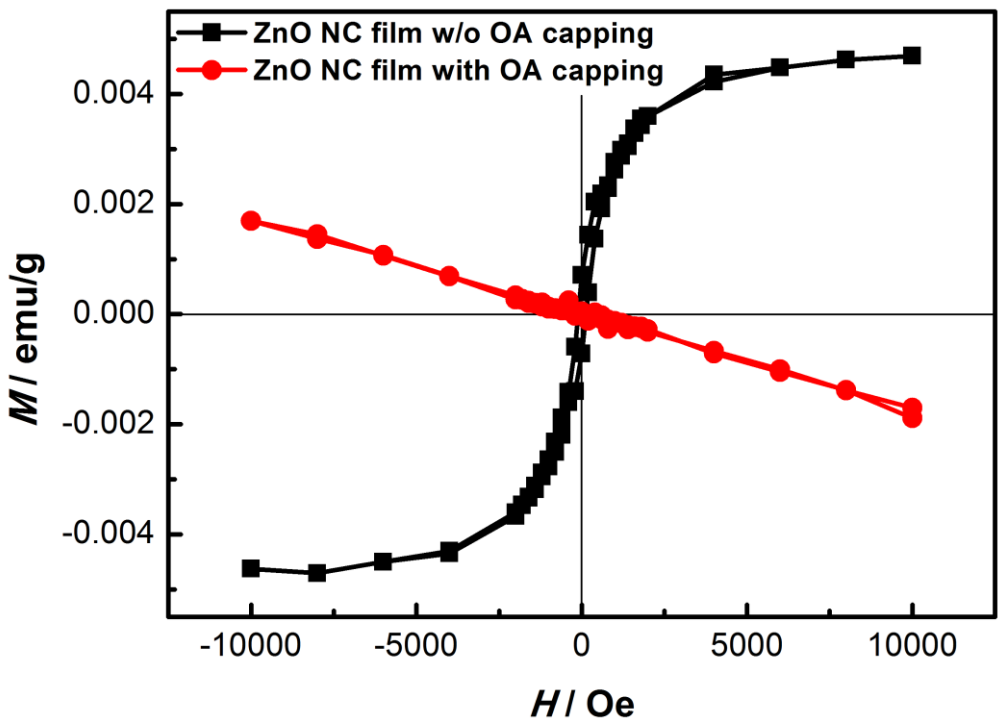

Fig. S13 300 K magnetization contrast between spin-coated ZnO NC film before and after OA capping, annealed at 400°C. Evidently, d^0-FM can be totally compensated under the presence of OA ligands.

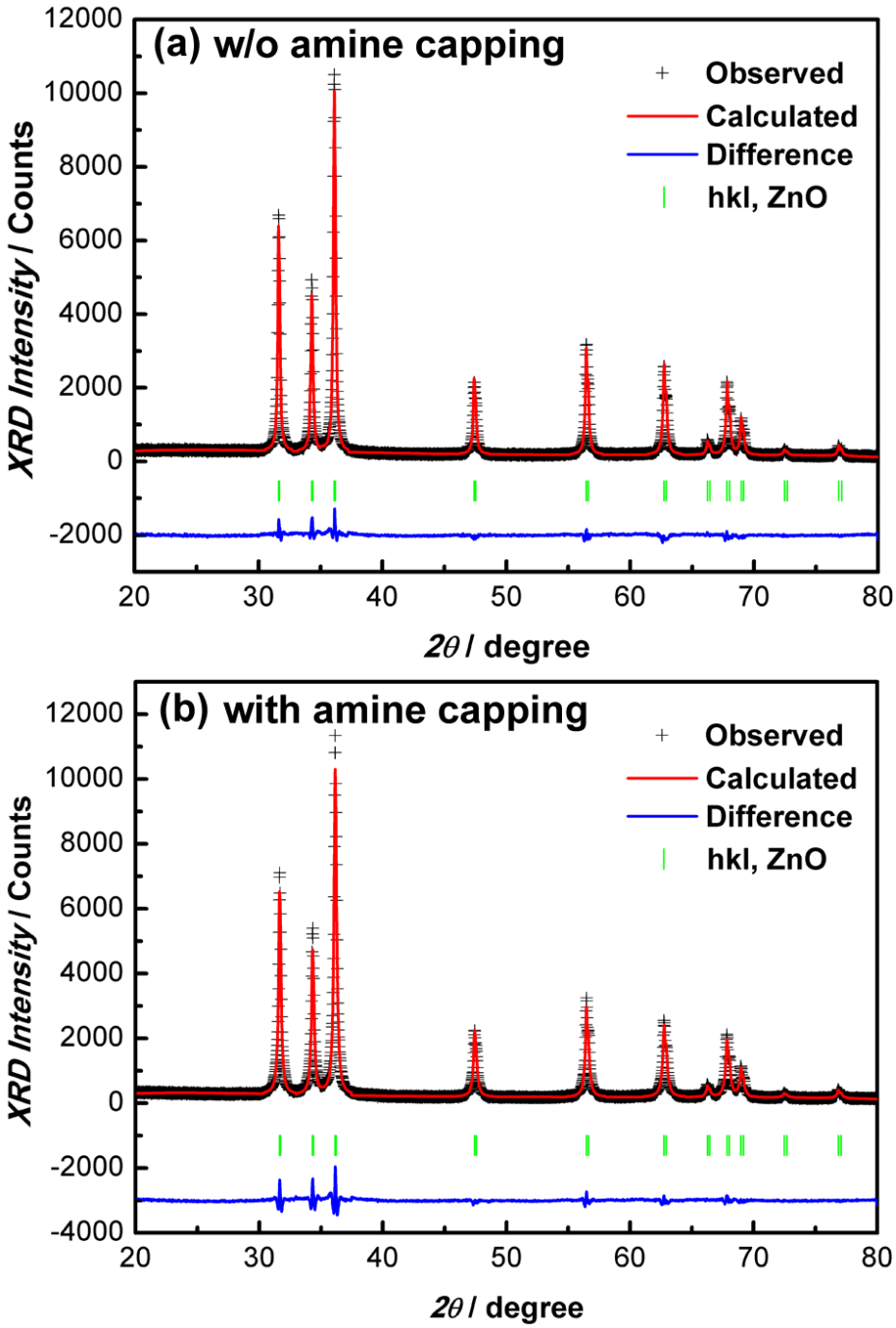

Fig. S14 The effect of amine-capping on texture in 400°C annealed 0.2% Cu-doped ZnO nanocrystalline film.

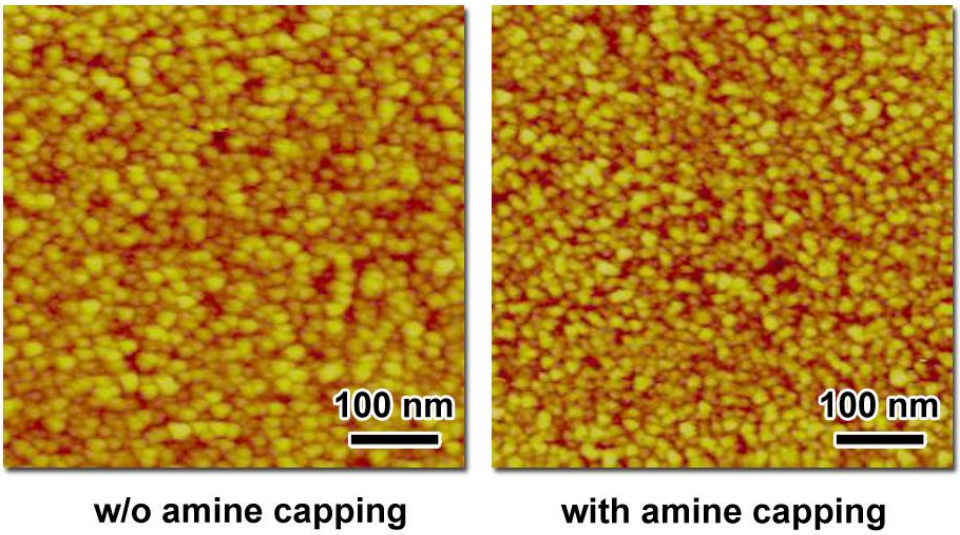

Fig. S15 The effect of amine-capping on grain-size in 400°C annealed 0.2% Cu-doped ZnO nanocrystalline film.

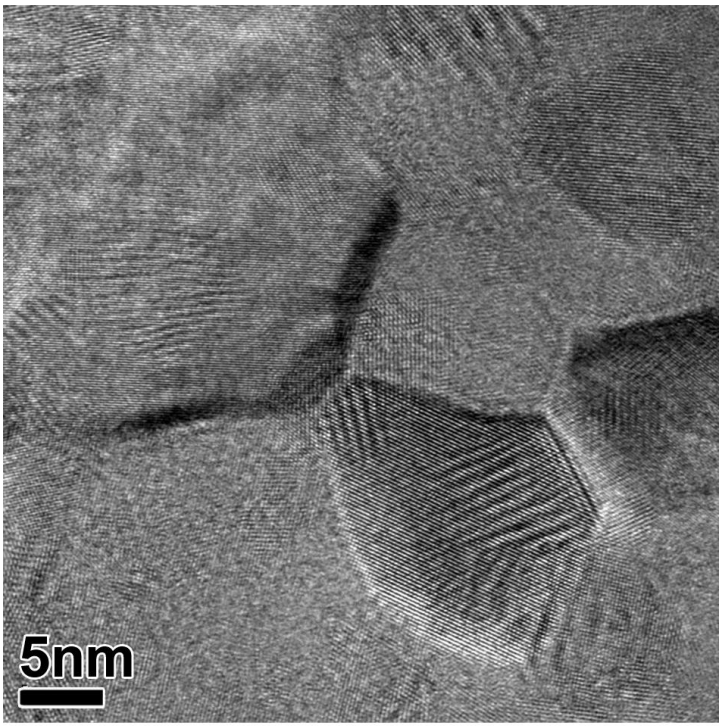

w/o amine capping

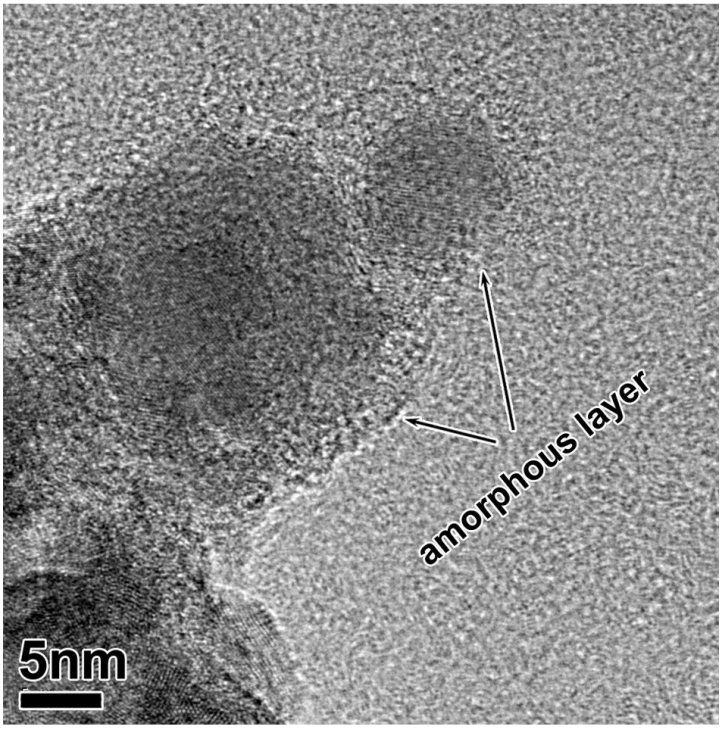

with amine capping

Fig. S16 The effect of amine-capping on amorphous layer in 400°C annealed 0.2% Cu-doped ZnO nanocrystalline film.

References

1. G. Z. Xing, J. B. Yi, J. G. Tao, T. Liu, L. M. Wong, Z. Zhang, G. P. Li, S. J. Wang, J. Ding, T. C. Sum, C. H. A. Huan and T. Wu, *Adv. Mater.*, 2008, 20, 3521-3527.
2. H. J. Xu, H. C. Zhu, X. D. Shan, Y. X. Liu, J. Y. Gao, X. Z. Zhang, J. M. Zhang, P. W. Wang, Y. M. Hou and D. P. Yu, *J. Phys.: Condens. Matter*, 2010, 22, 016002.
3. J. H. Zheng, J. L. Song, X. J. Li, Q. Jiang and J. S. Lian, *Cryst. Res. Technol.*, 2011, 46, 1143-1148.
4. Q.-Y. Xu, X.-H. Zheng and Y.-P. Gong, *Chinese Phys. B*, 2010, 19.
5. H. Liu, J. Yang, Z. Hua, Y. Zhang, L. Yang, L. Xiao and Z. Xie, *Appl. Surf. Sci.*, 2010, 256, 4162-4165.
6. C. C. Lin, S. L. Young, C. Y. Kung, H. Z. Chen, M. C. Kao, L. Horng and Y. T. Shih, *IEEE. T. Magn.*, 2011, 47, 3366-3368.
7. P. K. Sharma, R. K. Dutta and A. C. Pandey, *J. Magn. Magn. Mater.*, 2009, 321, 4001-4005.
8. S. Yılmaz, E. McGlynn, E. Bacaksız, S. Özcan, D. Byrne, M. O. Henry and R. K. Chellappan, *J. Appl. Phys.*, 2012, 111, 013903.
9. C. Xu, K. Yang, L. Huang and H. Wang, *J. Chem. Phys.*, 2009, 130, 124711.
10. J. Huang, L. P. Zhu, L. Hu, S. J. Liu, J. Zhang, H. H. Zhang, X. P. Yang, L. W. Sun, D. H. Li and Z. Z. Ye, *Nanoscale*, 2012, 4, 1627-1635.
11. H.-J. Lee, B.-S. Kim, C. R. Cho and S.-Y. Jeong, *Phys. Status Solidi B*, 2004, 241, 1533-1536.
12. X. Wang, J. B. Xu, W. Y. Cheung, J. An and N. Ke, *Appl. Phys. Lett.*, 2007, 90, 212502.
13. M. Shuai, L. Liao, H. B. Lu, L. Zhang, J. C. Li and D. J. Fu, *J. Phys. D: Appl. Phys.*, 2008, 41, 135010.
14. T. S. Herng, S. P. Lau, S. F. Yu, H. Y. Yang, X. H. Ji, J. S. Chen, N. Yasui and H. Inaba, *J. Appl. Phys.*, 2006, 99, 086101.
15. T. S. Herng, S. P. Lau, S. F. Yu, H. Y. Yang, K. S. Teng and J. S. Chen, *J. Phys.: Condens. Matter*, 2007, 19, 356214.
16. T. S. Herng, S. P. Lau, S. F. Yu, J. S. Chen and K. S. Teng, *J. Magn. Magn. Mater.*, 2007, 315, 107-110.
17. L. Q. Zhang, Z. Z. Ye, J. G. Lu, B. Lu, Y. Z. Zhang, L. P. Zhu, J. Zhang, D. Yang, K. W. Wu, J. Huang and Z. Xie, *J. Phys. D: Appl. Phys.*, 2010, 43, 015001.
18. G. Shukla, *Appl. Phys. A*, 2009, 97, 115-118.
19. A. Tiwari, M. Snure, D. Kumar and J. T. Abiade, *Appl. Phys. Lett.*, 2008, 92, 062509.
20. D. Chakraborti, G. R. Trichy, J. T. Prater and J. Narayan, *J. Phys. D: Appl. Phys.*, 2007, 40, 7606-7613.
21. D. Chakraborti, J. Narayan and J. T. Prater, *Appl. Phys. Lett.*, 2007, 90, 062504.

22. T. Herng, D. C. Qi, T. Berlijn, J. Yi, K. Yang, Y. Dai, Y. Feng, I. Santoso, C. Sánchez-Hanke, X. Gao, A. Wee, W. Ku, J. Ding and A. Rusydi, *Phys. Rev. Lett.*, 2010, 105, 207201.
23. D. B. Buchholz, R. P. H. Chang, J. H. Song and J. B. Ketterson, *Appl. Phys. Lett.*, 2005, 87, 082504.
24. S. Y. Zhuo, X. C. Liu, Z. Xiong, J. H. Yang and E. W. Shi, *Solid State Commun.*, 2012, 152, 257-260.
25. C. O. Kim, S. Kim, H. T. Oh, S.-H. Choi, Y. Shon, S. Lee, H. N. Hwang and C.-C. Hwang, *Physica B*, 2010, 405, 4678-4681.
26. D. L. Hou, X. J. Ye, H. J. Meng, H. J. Zhou, X. L. Li, C. M. Zhen and G. D. Tang, *Appl. Phys. Lett.*, 2007, 90, 142502.
27. D. L. Hou, X. J. Ye, X. Y. Zhao, H. J. Meng, H. J. Zhou, X. L. Li and C. M. Zhen, *J. Appl. Phys.*, 2007, 102, 033905.
28. Z. Ahmed Khan and S. Ghosh, *Appl. Phys. Lett.*, 2011, 99, 042504.
29. C. Sudakar, J. S. Thakur, G. Lawes, R. Naik and V. M. Naik, *Phys. Rev. B*, 2007, 75.
30. T. Li, H. Fan, J. Yi, T. S. Herng, Y. Ma, X. Huang, J. Xue and J. Ding, *J. Mater. Chem.*, 2010, 20, 5756-5762.
31. Z. F. Wu, X. M. Wu, L. J. Zhuge, X. M. Chen and X. F. Wang, *Appl. Phys. Lett.*, 2008, 93, 023103.